

# Spin-isospin nuclear response using the existing microscopic Skyrme functionals

S. Fracasso and G. Colò

*Dipartimento di Fisica, Università degli Studi and INFN,  
Sezione di Milano, 20133 Milano, Italy*

## Abstract

Our paper aims at providing an answer to the question whether one can reliably describe the properties of the most important spin-isospin nuclear excitations, by using the available non-relativistic Skyrme energy functionals. Our method, which has been introduced in a previous publication devoted to the Isobaric Analog states, is the self-consistent Quasiparticle Random Phase Approximation (QRPA). The inclusion of pairing is instrumental for describing a number of experimentally measured spherical systems which are characterized by open shells. We discuss the effect of isoscalar and isovector pairing correlations. Based on the results for the Gamow-Teller resonance in  $^{90}\text{Zr}$ , in  $^{208}\text{Pb}$  and in few Sn isotopes, we draw definite conclusions on the performance of different Skyrme parametrizations, and we suggest improvements for future fits. We also use the spin-dipole resonance as a benchmark of our statements.

PACS numbers: 21.10.Re, 21.30.Fe, 21.60.Jz, 21.10.Hw, 24.30.Cz, 25.40.Kv

## I. INTRODUCTION

The special role played by the spin-isospin modes for the detailed understanding of the structure of nuclei has been pointed out since several decades. The subject has been treated in review papers [1] and textbooks [2]. Spin-isospin transitions can occur spontaneously, in the case of  $\beta$ -decay. The simplest case is that of the Gamow-Teller (GT) transitions, whose corresponding operator is

$$\vec{O}_{GT\pm} = \sum_{i=1}^A \vec{\sigma}(i) t_{\pm}(i). \quad (1)$$

This operator is associated with a model-independent sum rule, namely  $m_0 \equiv m_0(t_-) - m_0(t_+) = 3(N - Z)$  where  $m_0(t_{\pm})$  is the total strength in the given channel. Since the early work of K. Ikeda *et al.* where this sum rule has been introduced [3], it has been clear that in the limited energy window accessible to the  $\beta$ -decay only a limited fraction of this sum rule can be found. A collective state should be expected at higher energy, and this Gamow-Teller resonance (GTR) has been indeed detected in (p,n) experiments starting from the mid-seventies [4]. Later, systematic ( ${}^3\text{He},\text{t}$ ) experiments which are characterized by much better energy resolution have also been performed. We should remind that in nuclei having neutron excess the Ikeda sum rule is exhausted almost entirely by states in the  $t_-$  channel as the Pauli principle hinders the  $t_+$  excitations.

In medium-heavy nuclei, ranging from  ${}^{90}\text{Zr}$  to  ${}^{208}\text{Pb}$ , the GTR is located somewhat above the Isobaric Analog Resonance (IAR) which is also well known from (p,n) and ( ${}^3\text{He},\text{t}$ ) experiments. This corresponds to the typical energy region of the giant resonances, that is, 10-20 MeV (we refer here to energies with respect to the ground state of the mother, or target, nucleus). At the same time, the main GT peak(s) turns out to exhaust only about 50% of the Ikeda sum rule in these medium-heavy nuclei; this percentage becomes about 70% if the whole strength in the neighboring energy region (i.e., below  $\approx 20$  MeV in the daughter, or final, nucleus) is collected [5].

The extraction of the strength from the measured cross sections is far from being straightforward. However, due to their  $\Delta L=0$  character, the GTR and IAR angular distributions are strongly peaked at  $0^\circ$ , and an approximate proportionality between the zero-degree cross section and the strength has been found under the hypothesis of high incident energy, zero momentum transfer and neglect of the non-central components of the projectile-target interaction [6].

The problem of the so-called “missing GT strength” has considerably attracted the attention of nuclear physicists. Some theorists have speculated that part of the missing GT strength should be found at very high excitation energy ( $\approx 300$  MeV) due to the coupling with the internal  $1^+$  excitation of the nucleon, i.e., the  $\Delta$ -isobar (1232 MeV): the reader can consult the references quoted in [1]. In other calculations [7], it has been shown that the usual coupling of the one particle-one hole (1p-1h) configurations involved in the GTR with two particle-two hole (2p-2h) configurations is able to shift strength outside the range accessible to experiments and explain in a more conventional fashion the missing strength. Experimentally, from the multipole-decomposition analysis (MDA) of the cross sections measured in the  $^{90}\text{Zr}(p,n)$  experiment at  $E_p=295$  MeV [8], it has been argued that 90% of the GT strength can be recovered below 50 MeV excitation energy, leaving little room for the coupling with the  $\Delta$ -isobar. However, part of the analysis (for instance, the estimate of the isovector monopole contribution) has been somehow questioned.

The coupling of simple 1p-1h configurations with more complex one, and the high-lying GT strength, are not the issue of the present paper. Using the Skyrme Hamiltonian, the GTR in  $^{208}\text{Pb}$  has been calculated, beyond simple RPA, taking into account the coupling with the continuum as well as with configurations made up with a p-h pair coupled with a collective vibration [9]. This calculation has been able to reproduce the values of the branching ratios associated with the proton decay of the GTR; at the same time, it has been shown that the position of the main GT peak does not change too much with respect to simple RPA. In Figs. 4 and 5 of Ref. [9] one can see that the peak is indeed shifted downwards by few hundreds of keV. The calculations reported in Ref. [10] (also based on the coupling with phonons) are much more phenomenological, but the result is similar. The redistribution of strength mentioned in the previous paragraph is instead quite sizeable and this point should be kept in mind for the following discussion. No such complete and fully microscopic calculation, at the level of four-quasiparticle coupling, is available for the charge-exchange modes in open shell systems. We still need, and this is our first aim here, to assess in a clear way the properties of the Skyrme functionals, complemented by an effective pairing force, in the spin-isospin channel by studying the corresponding excitations within the self-consistent mean-field framework. As self-consistent calculations, we mean Quasiparticle Random Phase Approximation (QRPA) calculations based on a Hartree-Fock plus Bardeen-Cooper-Schrieffer (HF plus BCS) description of the ground state. Our model

has been introduced and applied to the IAR in Ref. [11]. Some rather preliminary results using the same model have been presented in Conference proceedings [12].

There are not many self-consistent QRPA calculations available. The proton-neutron QRPA based on Skyrme forces in the particle-hole (p-h) channel (with a simplified form, i.e., with a separable approximation), and on the use of a constant pairing gap in HF-BCS plus a free residual particle-particle (p-p) interaction, has been intensively applied to the study of both spherical and deformed nuclei [13]. The issue is to know to what extent intrinsic deformations affect the measured  $\beta$ -decay spectra and the authors of [13] have explored many isotopic chains, including heavy ones [14]. Later, the first attempt to implement a self-consistent QRPA scheme based on HFB has been made in Ref. [15], which is another work devoted to  $\beta$ -decay (in this case limited to spherical isotopes – lying on the  $r$ -process nucleosynthesis path). The same group has studied the high-lying GTR, and the behavior of different Skyrme parameter sets [16]: we will discuss in detail, in what follows, the comparison of that work with the present one. The charge-exchange modes have also been attacked by using relativistic charge-exchange RPA and QRPA [17, 18, 19, 20].

But, aside from the mentioned ones, most of the QRPA calculations are not self-consistent. To study the GTR in  $^{208}\text{Pb}$ , the quasiparticle-phonon model has been employed in Ref. [21], and the so-called Pyatov method in Ref. [22]. Most of the systematic calculations (done also for open-shell nuclei and/or for the  $\beta$ -decay) are rather based on some empirical mean field (e.g., Woods-Saxon) and residual interaction depending, in the spin-isospin channel, on a parameter  $g'_0$ . A schematic model of this type can certainly be useful in many respects. As we discuss below, predictions of the schematic RPA model based on these simple phenomenological ingredients can be regarded as a guideline while understanding our results. However, we stick on the idea of a full microscopic approach. This is of special interest nowadays: if new radioactive beam facilities aim at studying spin-isospin properties of the exotic systems, constraining this channel in the microscopic Hamiltonian must be envisaged, while sticking on phenomenological inputs may be not appropriate.

The study of spin-isospin excitations is not only of interest for nuclear structure, but also for particle physics or astrophysics. In fact, the detailed knowledge of spin-isospin nuclear matrix elements (with  $\approx 20\%$  accuracy) is required to extract from the  $\beta\beta$ -decay experimental findings the hierarchy of neutrino masses. And, in the astrophysical sector, the details of the  $r$ -process nucleosynthesis can be understood, once more, only if nuclear

masses, photonuclear cross sections and  $\beta$ -decay probabilities are precisely known. Last but not least, we mention the importance of knowing the neutrino-nucleus interactions in different contexts (from the stellar environment, to the case of materials which are used for crucial experiments on the neutrinos). All these motivations lie at the basis of the recent works concerning the spin-isospin nuclear modes.

In the present work, as compared with Ref. [16], we re-discuss in particular the role of the so-called spin-gradient (or  $J^2$ ) terms of the Skyrme energy functionals, and we find somewhat different results for the GT strength distributions. Moreover, we perform a more general analysis since we also study the role of the pairing residual interaction (which has been neglected in [16]), and we devote some attention to the case of another kind of spin-isospin excitation, namely the isovector spin-dipole resonance.

The isovector spin-dipole (IVSD) resonance is excited by the operator

$$O_{IVSD\pm,J^\pi} = \sum_{i=1}^A r_i \left[ \vec{Y}_1(\hat{r}_i) \otimes \vec{\sigma}(i) \right]_{J^\pi M} t_\pm(i), \quad (2)$$

where  $J^\pi = 0^-, 1^-, 2^-$ . The charge-exchange experimental measurements, whether (p,n) or ( ${}^3\text{He},\text{t}$ ), show indeed evidence of  $L \neq 0$  strength. Most of this strength is very fragmented, and an unambiguous signature for the different multipoles (monopole, dipole etc.) is still missing. In theoretical calculations, the spin-dipole distributions look quite broad, also because of the presence of three  $J^\pi$  components. Some calculations for magic nuclei have been available for long time: the reader can refer to the phenomenological calculations of Ref. [23] or to the HF plus continuum-RPA of Ref. [24]. Recently, there has been new interest in the study of this channel: some low-lying transitions which are important for the  $\beta\beta$ -decay have in fact first-forbidden character, and the reliability of theoretical models in predicting properties of  $L \neq 0$  charge-exchange transitions is under discussion. Moreover, it has been suggested that the precise determination of the IVSD sum rule (analogous to the Ikeda sum rule) can be a unique probe of the neutron skins, as it is proportional to  $N\langle r^2 \rangle_n - Z\langle r^2 \rangle_p$  [25]. Since it would be highly desirable to extract the key parameters governing the asymmetry part of the nuclear equation of state from the difference of the neutron and proton radii, and the experimental determination of neutron radii by means of scattering data is not very accurate, this alternative way of extracting the same quantity is potentially of great interest (see also [26]). In the spirit of the present investigation, it is important of course to establish whether the conclusions about the robustness of the Skyrme-QRPA with given parameter

sets, remain valid when another multipolarity is studied.

The outline of our paper is the following. We first provide the basic information about our formalism in Sec. II, by limiting ourselves to what is essential for understanding the rest of the discussion. One part of the Skyrme functionals that we employ here, namely that associated with the so-called  $J^2$  terms, has been discussed recently, also in Ref. [16]; for this reason, we discuss at length the point of view emerging from our calculations and results in Sec. III. We can then analyze the results for the GT and IVSD strength distributions, respectively, in Secs. IV and V, and draw relevant conclusions on the performances of the existing Skyrme sets as well as make suggestions for the future fits. Considerations on the pairing correlations are made in Sec. VI, before coming to the overall conclusions of Sec. VII.

## II. FORMALISM

Our model has been introduced in Ref. [11] and we will focus here only on those aspects which are important for the understanding of our results. We start by dealing with the HF-BCS coupled problem, that is, at each iteration we solve in real space the HF equations and the BCS gap and number equations. For  $^{90}\text{Zr}$  and  $^{208}\text{Pb}$  pairing is neglected. For the Sn isotopes, the pairing window is the 50-82 neutron shell, and the pairing force is the same which has been fitted in Ref. [11], namely a zero-range, density-dependent interaction of the type

$$V = V_0 \left( 1 - \left( \frac{\rho \left( \frac{\vec{r}_1 + \vec{r}_2}{2} \right)}{\rho_C} \right)^\gamma \right) \cdot \delta(\vec{r}_1 - \vec{r}_2), \quad (3)$$

with  $V_0=680 \text{ MeV}\cdot\text{fm}^3$ ,  $\rho_C=0.16 \text{ fm}^{-3}$  and  $\gamma=1$ . It has been checked that when this pairing force is used in connection with different Skyrme forces (we consider in this work the parameter sets SIII [27], SGII [28], SLy5 [29] and SkO' [30]), the resulting pairing gaps do not vary too much along the Sn isotope chain.

All the states at positive energy (either those in the BCS pairing window or those outside this window, which have occupation factors  $v^2$  equal to zero) are calculated using box boundary conditions: that is, our continuum is discretized. Two quasiparticle configurations (or particle-hole, in the cases in which pairing is absent) with proper  $J^\pi$  are built and the

QRPA matrix equations,

$$\begin{pmatrix} A & B \\ -B & -A \end{pmatrix} \begin{pmatrix} X^{(n)} \\ Y^{(n)} \end{pmatrix} = E_n \begin{pmatrix} X^{(n)} \\ Y^{(n)} \end{pmatrix}, \quad (4)$$

are solved in this model space. The upper limit for the configurations is chosen so that the results are stable against variations and the proper sum rules, which are expected to hold in full self-consistent calculations, are indeed exhausted with high accuracy. In the charge-exchange case, it is known that these sum rules are the difference of the non energy-weighted sum rules in the two isospin channels  $m_0 \equiv m_0(t_-) - m_0(t_+)$ , and the sum of the energy-weighted sum rules  $m_1 \equiv m_1(t_-) + m_1(t_+)$ . The analytic values of these sum rules in the case of the Skyrme forces can be found, e.g., in Ref. [31].

In the p-h channel, for the charge-exchange modes, the residual interaction reads

$$v^{ph}(\mathbf{r}_1, \mathbf{r}_2) = \delta(\mathbf{r}_1 - \mathbf{r}_2) \left[ v_{01}(r) + v_{11}(r) + v'_{01} + v'_{11} + v_1^{(s.o.)} \right]. \quad (5)$$

In this formula, the two indices for each of the first four terms in square brackets refer to the projection in a given  $\sigma\tau$ -channel. The terms with (without) a prime are those which are (are not) velocity-dependent. The last term is the isovector part of the spin-orbit residual interaction.

In the following of this work, our considerations will focus on the spin-isospin terms of the p-h residual interaction, the spin-independent terms being far from dominant or even not active. For the sake of completeness, we provide anyway the detailed expressions of all terms:

$$\begin{aligned} v_{01}(r) &= 2C_1^\rho [\rho(r)] \vec{\tau}_1 \vec{\tau}_2, \\ v_{11}(r) &= 2C_1^S [\rho(r)] \vec{\sigma}_1 \vec{\sigma}_2 \vec{\tau}_1 \vec{\tau}_2, \\ v'_{01} &= \left[ (k'^2 + k^2) \frac{1}{2} (C_1^\tau - 4C_1^{\Delta\rho}) + k'k (3C_1^\tau + 4C_1^{\Delta\rho}) \right] \vec{\tau}_1 \vec{\tau}_2, \\ v'_{11} &= \left[ (k'^2 + k^2) \frac{1}{2} (C_1^T - 4C_1^{\Delta S}) + k'k (3C_1^T + 4C_1^{\Delta S}) \right] \vec{\sigma}_1 \vec{\sigma}_2 \vec{\tau}_1 \vec{\tau}_2, \\ v_1^{(s.o.)} &= -2iC_1^{\nabla J} (\sigma_1 + \sigma_2) k' \times k \vec{\tau}_1 \vec{\tau}_2. \end{aligned} \quad (6)$$

We remind that

$$\begin{aligned} k' &= -\frac{1}{2i} (\nabla'_1 - \nabla'_2), \\ k &= \frac{1}{2i} (\nabla_1 - \nabla_2), \end{aligned} \quad (7)$$

with the operators acting at right (left) in the case of  $k$  ( $k'$ ). The parameters entering the above expressions can be written in terms of those of the Skyrme force. For the convenience of the reader, this correspondence is explicitly provided in the Appendix.

In the p-p channel, we fix self-consistently the residual isovector pairing force by exploiting the isospin symmetry, that is, we take the isovector proton-neutron pairing interaction to be the same as the neutron-neutron one used in the BCS description of the ground state. The proton-neutron isoscalar pairing cannot be constrained: presently, we miss a clear indication from empirical data about the parameter of the isoscalar pairing force. Using a quite conservative approach, we present in the following results which, unless otherwise stated, correspond to an isoscalar pairing force equal to the isovector one. We have tried to give some indication about the sensitivity of our results when in the isoscalar channel a strength  $V_0^{(T=0)}$  different from  $V_0^{(T=1)}$  is adopted. This kind of study has been done in connection with the RMF analysis of the charge-exchange modes. No such analysis has been available so far in the case of the Skyrme calculations; we have found results which are to some extent consistent with those associated with the RMF study. In that case, a finite-range Gogny pairing force is employed, but this does not seem to produce macroscopic differences with respect to the use of zero-range effective pairing forces.

### III. TREATMENT OF THE $J^2$ TERMS OF THE ENERGY FUNCTIONAL

As mentioned above, the energy functional includes the so-called spin-gradient, or  $J^2$ , terms which are built on the spin-orbit densities. They arise from the exchange part of the central Skyrme interaction [32]. The spin-orbit densities vanish in the ground state of spin-saturated nuclei but they provide a contribution to the spin and spin-isospin parts of the residual p-h interaction. In the past (with some exceptions), the  $J^2$  terms have been neglected when fitting the Skyrme parameters; some more recent parametrizations include them, and in particular we will consider in the following the sets SLy5 and SkO'. In the discussion below, for the sake of simplicity, we will call type I-forces the Skyrme sets which do not include the  $J^2$  terms in the fit, and type II-forces those which do include them. To our knowledge, there is not a clear indication emerging from the nuclear phenomenology whether these  $J^2$  terms must be included in a physically sound energy functional. Of course, if the functional is derived from a two-body force of the Skyrme type, which has a momentum

dependence, it looks questionable to drop the  $J^2$  terms. We should also notice that the  $J^2$  terms neither are hard to evaluate, nor they are time-consuming if the HF calculation is performed in coordinate space as in the present case.

In the past many RPA calculations have been performed with type I-forces. The authors of [16] have pointed out that those calculations (e.g., those of Ref. [28]) do not respect the full self-consistency, since the contributions from the  $J^2$  terms are included in the residual interaction but not in the mean field (the authors of [28] have also neglected the spin-orbit residual interaction but this has practically no effect). To respect the Galilean invariance, the authors of [16], when employing type I-forces in their work, have adopted the prescription of removing from the residual interaction not only the contribution from the  $J^2$  term, but also that from the so-called  $S \cdot T$  term in the functional. This amounts to setting  $C_1^T$  equal to zero (cf. Eq. (6)) and leads to a substantial quenching of the velocity-dependent part in the spin-isospin channel since  $C_1^{\Delta S}$  is not as large. Therefore, we deem that the issue should be further discussed here.

We start from the fact that fitting the Skyrme parameters is usually done by using, in addition to nuclear (or neutron) matter quantities, binding energies and charge radii of few selected isotopes (with the spin-orbit strength  $W_0$  separately adjusted). In  $^{208}\text{Pb}$ , the binding energy (charge radius) changes by 0.22% (0.15%), using the force SLy4, when the  $J^2$  terms are omitted or inserted. These variations are too small to allow a clear statement about the manifestation of the  $J^2$  terms in the benchmarks used for the fit because it must be noted that in the protocol for the parameter fitting presented in Ref. [29], larger errors on binding energies and charge radii are imposed in the  $\chi^2$ -formula to let the fit converge (we mean here, larger than the experimental error bars and larger than the  $\approx 0.1\text{-}0.2\%$  variations we just mentioned). Even in  $^{120}\text{Sn}$ , which is not used for the parameter fitting but is studied in the present paper, we find a similar pattern.

On the other hand, the effect of the  $J^2$  terms on the single-particle spectrum becomes appreciable. In Fig. 1 we display the highest occupied and lowest unoccupied proton and neutron levels in  $^{208}\text{Pb}$ . With few exceptions the spectra of SLy4 and SLy5 are similar, the proton (neutron) levels being in general slightly lower (higher) in energy in the case of SLy4. The spectrum associated with SLy4 plus the  $J^2$  terms is instead somewhat different: in fact, one notices that the  $j_>$  ( $j_<$ ) spin-orbit partners are raised (lowered) in energy, both for protons and neutrons, up to 400 keV. Accordingly, the unperturbed energies of the  $j_> \rightarrow j_<$

configurations are reduced. The net overall effect is that the main GTR peak varies only by 60 keV between SLy4 and SLy5, but it varies by 0.5 MeV when the  $J^2$  terms are added to the SLy4 mean field. This is due to the fact that only  $j_> \rightarrow j_<$  configurations are present in the GTR wavefunction calculated with the Lyon parameter sets. We show the variation of the GTR peak energy along the Sn isotopes in Fig. 2. A stronger effect of the  $J^2$  terms is that associated with the spin-isospin residual p-h force. In fact, if we remove the part corresponding to the  $J^2$  term in the energy functional from the p-h interaction, the GTR peak energy changes by about 2 MeV. Qualitatively similar conclusions can be deduced from the study of the Sn isotopes.

This detailed study led us to the following conclusions. The  $J^2$  terms do not manifest themselves so much in the ground state observables used for the fit of the Skyrme parameters, but they do affect some other properties of the nuclear ground state like the spin-orbit splitting. Moreover, they play a major role when GT calculations are performed, mainly because of their contribution to the p-h interaction. Looking at our results, we believe that the most natural and physical choice is to omit the contribution of the  $J^2$  terms when calculating the ground state with type-I forces, but retain the corresponding contribution in the residual p-h force. In the case of nuclei which are not spin-saturated, we agree with the authors of [16] that this choice breaks self-consistency. If one insists on self-consistency, the choice of inserting the  $J^2$  contribution in the ground state alters the GTR energy by about 0.5 MeV, whereas the alternative choice of neglecting the  $J^2$  contribution systematically appears to be quite unnatural. After all, we definitely suggest that fits of new Skyrme parameters are systematically done by inserting the  $J^2$  terms.

We conclude this Section by mentioning that in the recent literature there have been claims about the necessity of complementing the usual Skyrme forces with tensor terms (even and odd). Together with other collaborators, the authors of the present paper have shown that the contribution of the tensor effective force can remedy serious and qualitative discrepancies between the single-particle levels predicted within the Skyrme framework and those which are experimentally observed [33]. Similar discussions can be found in [34]. The reason for mentioning this here, is that the two-body zero-range tensor force gives the same kind of contribution to the mean field of even-even nuclei nuclei as the  $J^2$  terms. Consequently, the tensor force will affect the GT centroid energy, and we have estimated its impact by using sum rule arguments in [33]. Since the aim of this work is the discussion

of the performance of the existing functionals we do not come back to this point in the following. If a new general fit of Skyrme functionals plus tensor contribution is made, and the corresponding (Q)RPA becomes available, new steps can be undertaken.

#### IV. RESULTS FOR THE GAMOW-TELLER RESPONSE

As stated in the Introduction, the strength distributions associated with the Gamow-Teller operator  $\sum_{i=1}^A \vec{\sigma}(i)t_-(i)$  are expected to display a main resonance located at energy  $E_{\text{GTR}}$ . In Fig. 3 we show the behavior of  $E_{\text{GTR}} - E_{\text{IAR}}$ , where  $E_{\text{IAR}}$  is the isobaric analog energy, as function of  $(N - Z)/A$ . Experimental data are from Refs. [35, 36, 37]. The theoretical (Q)RPA calculations have been performed with some of the most recent and/or widely used Skyrme interactions, that is, SIII, SGII, SLy5 and SkO'. For SIII and SGII, on ground of what discussed in the previous Section, the  $J^2$  terms are included in the residual interaction and not in the mean field. When our calculations produce a resonance which is fragmented in more than one peak, the exact definition of the values of  $E_{\text{GTR}}$  used in the figure is the centroid  $m_1/m_0$  where the two sum rules are evaluated in the interval of the resonance. This interval is 15-24 MeV for Pb and 12-22 MeV for the Sn isotopes (in Zr, there is a single GT main state). In some cases, we face the well-known problem of (Q)RPA instabilities and (Q)TDA values are reported (in particular, this happens for  $^{90}\text{Zr}$  and  $^{118,120}\text{Sn}$  when the force SkO' is employed, and for  $^{114}\text{Sn}$  when using SGII). In Ref. [11] we have shown that our model provides quite accurate values of  $E_{\text{IAR}}$  but in the figure, for simplicity, we have used the experimental values for this quantity.

From Fig. 3, we can draw two first conclusions. First, one should notice that the linear behavior of  $E_{\text{GTR}} - E_{\text{IAR}}$  vs.  $(N - Z)/A$  was already checked, on the experimental data, in [38] as it was expected on the ground of simple schematic models [1, 39]. In fact, if one performs a simple RPA calculation using a separable interaction in a restricted space (made up with the excess neutrons and the proton spin-orbit partners), one finds that

$$E_{\text{GTR}} - E_{\text{IAR}} = \Delta E_{ls} + 2 \frac{\kappa_{\sigma\tau} - \kappa_\tau}{A} (N - Z), \quad (8)$$

where  $\Delta E_{ls}$  is (an average value of) the spin-orbit splitting and  $\kappa_\tau/A$  ( $\kappa_{\sigma\tau}/A$ ) is the coupling constant of the separable schematic isospin (spin-isospin) residual force. The result of Fig. 3 suggests that our calculations, which are microscopically based and much more sophisticated,

obey in first approximation this simple pattern.

Besides that, one would also infer from the figure that some forces account better for the experimental findings while others perform less well. SkO' and SLy5 lie close to experiment, although their predictions drop below the experimental trend in  $^{208}\text{Pb}$ . SGII and SIII tend to overestimate the experimental energies but the trend of SGII does not change abruptly for  $^{208}\text{Pb}$ . The result obtained with the force SIII corresponds, within  $\approx 400$  keV, to the one found in Ref. [40]. The trend associated with the energy location of the GTR is not the only significant experimental observable: we should also analyze the fraction of  $m_0$ , or collectivity of the GTR.

In Figs. 4 and 5 we show the GT strength distributions, for  $^{208}\text{Pb}$  and  $^{120}\text{Sn}$ , respectively, associated with different forces. The strength functions in Sn display more fragmentation, as expected in keeping with its open-shell character. As mentioned in the Introduction, the experimental results is that about 60% of the total strength is exhausted by the GTR. In Table I we show the fraction of strength in the resonance region, for the different forces, both in the case of  $^{208}\text{Pb}$  (where the result obtained with the force SIII is very close to the 63.6% of Ref. [40]) and of few selected Sn isotopes. The results present a clear systematics: all forces concentrate  $\approx 60\text{-}70\%$  of the strength in the resonance region, apart from SLy5 (we remind again that our model does not include the coupling with 2p-2h).

Looking at the results for the GTR associated with the different forces, we ask ourselves if their performances depend more on the features of the associated mean field, or rather on the effective interaction in the spin-isospin channel, or on a delicate balance between the two ingredients. As far as the GTR energies are concerned, we did not find clear correlations between them and any simple parameter. On the other hand, interesting correlations are found if one analyzes the GT collectivity. This will allow us to draw quite strong conclusions about the Skyrme parameter sets under study.

In the cases of the three forces SIII, SGII and SkO' the wavefunctions are qualitatively similar, i.e., they display a large number of p-h components: the wavefunction associated to the main GT state, in the case of  $^{208}\text{Pb}$  and of the force SkO', is reported in Table II. The wavefunction resulting from SLy5, shown for the same nucleus in Table III, displays instead much less components. It has been checked that the reduced collectivity of the GTR calculated using SLy5 (and characteristic not only of Pb but of the Sn isotopes as well) cannot be explained simply in terms of the differences between the unperturbed energies associated

with this parameter set, as compared to the other ones. Indeed, we have observed that the p-h matrix elements of the SLy5 force are, on the average, smaller than those of the other forces.

In our analysis, we have also singled out the role of the velocity-dependent terms. In particular, we have observed that the  $(k'^2 + k^2)$  and the  $k'k$  contributions (cf. Eq. (6)) are comparable. If we drop these terms from the SLy5 p-h interaction, the GTR wavefunction becomes closer to that of the other forces, leading to an increase of the strength of  $\approx 20\%$  (the GT energy is of course also affected). In the case of the force SKO', the increase of collectivity when the velocity dependent terms are dropped, is extremely small. In fact, in the case of SkO', the coefficient  $C_1^T$ , characterized by a positive value of  $t_2$ , is smaller as compared with the other forces. We conclude that both the velocity-independent and velocity-dependent terms in the residual interaction are important.

This discussion already points out that, although it is not our purpose here to discuss in too much detail the strategy for improving the fits of effective Skyrme forces, we would like to strongly push forward the use of realistic constraints coming from the GT properties. We show in Fig. 6 direct correlations between the percentage of  $m_0$  associated with the GTR and combinations of Skyrme parameters (actually, we find correlation also with the  $t_1, t_2$  parameters separately and with the quantity  $\Theta_S$  defined in [29]). We are well aware that the  $(t_0, t_3)$  part of the interaction is mainly connected to the saturation properties of symmetric nuclear matter and the related value of the incompressibility, and the  $t_1, t_2$  part must be fitted together with finite nuclei ground state properties. The best choice should probably be to check *a posteriori* that the value of  $t_0$  and  $t_3$  are compatible with the upper panel of Fig. 6, and impose *a priori* the constraint associated with the lower panels on the  $t_1, t_2$  part, together with the other ones which are usually imposed. An alternative strategy is represented by the possibility of fixing the odd parameter  $C_1^T$  in an independent way with respect to the even part of the functional.

In some works, values of the Landau parameters have been fitted. Therefore, in Fig. 7 we show the correlation between the percentage of  $m_0$  exhausted by the GTR and either  $g'_0$  or  $g'_1$ . Future fits of Skyrme parameter sets can certainly also benefit from the use of one of these two constraints, which set either  $g'_0$  or  $g'_1$  around 0.45 or 0.5. We believe that this estimate is more appropriate than the one based on the empirical  $g'_0$  since this latter is, as a rule, extracted from calculations based on a Woods-Saxon mean field instead of a

Hartree-Fock one.

In summary, our results show clearly how the differences in the residual spin-isospin interaction (in particular in the velocity-dependent part), between various Skyrme parameter sets, manifest themselves if one studies the collectivity of the GTR. In particular, we point to the necessity of new fits which include the GT data as additional constraint, mainly to cure those forces like SLy5 which display a kind of anomaly in this respect.

Before concluding, we would like to show another kind of correlation with a physical parameter (cf. Fig 8). In fact, the GT collectivity is also related to the quantity which we denote by  $a_{\sigma\tau}$ . This quantity is analogous, in the spin-isospin case, to the well known asymmetry parameter  $a_\tau$  (we remind that sometimes notations like  $a_4$  or  $J$  are used for this latter quantity). It is

$$a_{\sigma\tau} = \frac{1}{2} \frac{\partial^2}{\partial \rho_{11}^2} \frac{E}{A}, \quad (9)$$

where we consider infinite matter with a generic spin and isospin asymmetry, and variations with respect to the spin-isospin density  $\rho_{11}$  defined as

$$\rho_{11} = \frac{\rho_{n\uparrow} - \rho_{n\downarrow} - \rho_{p\uparrow} + \rho_{p\downarrow}}{\rho}. \quad (10)$$

Although the spirit of our discussion is connected with the points raised in Ref. [16], our conclusions are different. In fact, we find different results than those published in [16]. We have tried to analyze in detail the sources of this difference and in particular we have checked the numerical effects in the case of  $^{90}\text{Zr}$  [41]. First, the energies in charge-exchange QRPA are naturally defined with respect to the target nucleus ground state. Since the experimental values of the charge-exchange resonances are provided in the final, or daughter, systems, we find quite straightforward (as we did in the past and as other authors do) to transform the experimental value into a corresponding value with respect to the target nucleus ground state by using experimental binding energies. However, this is not done in Ref. [16] where a theoretical estimate of the binding energy difference is carried out. In  $^{90}\text{Zr}$  the two alternative choices produce a discrepancy of 1.2 MeV. A second source of difference, already discussed, is the treatment of the  $J^2$  terms; in the case of  $^{90}\text{Zr}$ , this produce another  $\approx 1$  MeV of difference. After considering these two facts, part of the discrepancy (in  $^{90}\text{Zr}$ , another  $\approx 1$  MeV that is one third of the total discrepancy) has remained unexplained, and it is quite hard to attribute it simply to the different numerical implementations.

## V. RESULTS FOR THE SPIN-DIPOLE RESPONSE

The spin-dipole strength is not straightforward to be extracted experimentally. In absence of a well established proportionality between cross section at a given angle and dipole strength, either spectra subtraction or multipole decomposition analysis has to be attempted. On top of that, the three different  $J^\pi$  components are mixed: the similarity of the associated angular distributions would require sophisticated techniques to disentangle these components, like the use of polarized beams or the study of the  $\gamma$ -decay of the IVSD to the GTR and to low-lying states, performed with high energy resolution and high  $\gamma$ -ray detection efficiency [42].

Theoretically, a systematic clear picture of the IVSD is still missing. The two references mentioned in the Introduction [23, 24] predict, respectively, the IVSD in  $^{208}\text{Pb}$  to lie at 21.3 and 24.0 MeV. Only recently self-consistent calculations have been carried out in the same nucleus [40], but we have learnt from the previous discussion on the GTR that we need to consider several isotopes, and extract a global trend, if we wish to understand which interactions provide reliable results. Therefore, our present discussion is quite timely.

We of course can separate the three  $J^\pi$  components; however, to compare with experiment, we have to make a global average of the different  $J^\pi$  centroids. In particular, we estimate

$$\overline{E}_{IVSD-} = \frac{\sum_{J^\pi=0^-, 1^-, 2^-} m_1(J^\pi)}{\sum_{J^\pi=0^-, 1^-, 2^-} m_0(J^\pi)}, \quad (11)$$

for different nuclei. We evaluate the sum rules in the whole energy region where the transition strength is not negligible. We report the difference between these energies and the IAR energies in Fig. 9 and we compare with experimental data from Refs. [25, 39, 43].

It is rather satisfactory to have found that the different Skyrme forces behave quite similarly, as far as the IVSD is concerned, as they do for the simpler GTR. We have also looked in more detail to the strength distributions obtained by using the forces SkO' and SLy5. These distributions, for the nuclei  $^{208}\text{Pb}$  and  $^{120}\text{Sn}$  respectively, are displayed in Figs. 10 and 11 (SkO'), and in Figs. 12 and 13 (SLy5). The complete, or (Q)RPA, strength functions are shown in the upper panel and compared with the unperturbed strength functions which appear in the lower panel. The integral features of the distributions are resumed in Tables IV and V, for the two forces respectively. It is evident that the unperturbed centroids, whose values are reported in parenthesis, follow the known energy hierarchy [23], the  $2^-$  being the

lowest and the  $0^-$  the highest centroid. This is because the  $0^-$  wavefunctions are entirely composed by particle-hole (or two quasiparticles) excitations between proton-neutron states with opposite parity and the same total angular momentum, which are in general widely separated in energy. This trend is retained when the residual interaction is turned on, pushing up the centroids. The comparison between the unperturbed and the (Q)RPA distributions highlights the large values of the repulsive matrix elements of the residual interaction.

The IVSD spectra are rather fragmented. This fragmentation increases with the value of  $L$ , the  $2^-$  distribution being broader than the  $1^-$  and  $0^-$ . Due to the degeneracy factor, when the energy is averaged over the three spin-components, the contribution from  $0^-$  is less weighted than the  $1^-$  and  $2^-$ . It has been checked that the sum rules of  $2^-$ ,  $1^-$ ,  $0^-$  respect the ratio 5: 3: 1. In the  $2^-$  spectrum of  $^{208}\text{Pb}$ , it is possible to recognize a low-lying state, due to the  $\nu i_{13/2} \rightarrow \pi h_{9/2}$  particle-hole transition. Our findings are in reasonable agreement with the experimental peak observed, for the first time, at 2.8 MeV (6.5 MeV referred to the target ground state) in Ref. [44].

At this stage, it can be concluded that the behaviour of the considered Skyrme forces seems to be quite robust in reproducing properties of the isovector resonances which involve the spin-isospin degrees of freedom. Our results, reported in the figures and tables for different forces, can be compared with detailed forthcoming experimental findings (cf. e.g. [45]).

## VI. THE EFFECT OF ISOVECTOR AND ISOSCALAR PAIRING

In our calculations, we are in principle sensitive to the effect of both isovector and isoscalar pairing. We remind that the empirical evidence of isovector pairing, in the ground state of open-shell nuclei as well as in their low-lying excitations, has been clear for long time; but, in connection with microscopic calculations based on energy functionals, there is still debate about the proper pairing force (for instance, whether it should have volume, or surface, or mixed character). About isoscalar pairing, the situation is much less clear. The existence of a  $T = 0$  condensate has been questioned: if any, this is expected to show up only in the ground state of nuclei having equal number of protons and neutrons, or others lying very near. In our HF-BCS calculations, as stated in Sec. II, we fix the  $T = 1$  pairing force in order to have reasonable values for the empirical pairing gaps. The corresponding residual

p-p force has been fixed by using the isospin invariance. If we change its strength, even by producing a drastic change on the pairing gap, the energy of the GTR is only slightly affected ( $\approx 200$  keV). As already said, in keeping with the lack of possible constraints we vary the strength of the  $T = 0$  residual p-p interaction.

In the case of the GTR, that is, in the  $1^+$  channel, only the isoscalar residual pairing is active when a zero-range force is assumed. We have studied the effects of the pairing correlations on the GT strength distributions. We have found qualitatively similar outcomes in connection with different Skyrme forces. In the following, we will mention some specific results emerging from the calculations carried out using SLy5, just for illustrative purposes: since SLy5 does not produce highly collective GT states, the analysis of the effects produced by pairing is simpler, but our general conclusions will remain valid for other Skyrme sets.

The effect of the residual p-p isoscalar pairing is shown for the isotope  $^{118}\text{Sn}$  in Fig. 14: this effect is clearly visible, but it is small for the main peak which varies only by 300 keV when the pairing strength is changed from zero to a value equal to that of the  $T = 1$  pairing (i.e.,  $680 \text{ MeV}\cdot\text{fm}^3$ ). The IS pairing does not affect the total collectivity of the GTR, leaving the considerations made in Sec. IV basically unchanged.

In absence of residual pairing, two peaks appear above 15 MeV: the first one at 15.30 MeV is mainly due to the  $|\nu g_{9/2}, \pi g_{7/2}\rangle$  configuration while the second one at 18.47 MeV is dominated by the  $|\nu h_{11/2}, \pi h_{9/2}\rangle$  configuration. This so-called configuration splitting has been predicted [18, 46], but it is smaller than the spreading width of the GTR. The  $|\nu h_{9/2}, \pi h_{11/2}\rangle$  configuration gives a small QRPA solution at 18.68 MeV, which is not visible in the figure because of its negligible strength.

When the IS pairing is turned on, three new QRPA states show up, in which the mentioned configurations are mixed (cf. Table VI). The reduction of the configuration splitting (already remarked in [18], and which we have observed as a linear function of the pairing strength), and the mixing of spin-flip and back spin-flip configurations associated with the  $h$ -orbitals, can be understood by analyzing the matrix elements

$$\begin{aligned} V_{p_1 h'_2 p'_2 h_1}^{J,ph} &= \langle (p_1 h_1) J | V_{ph} | (p'_2 h'_2) J \rangle \left( u_{p_1} v_{h_1} u_{p'_2} v_{h'_2} + v_{p_1} u_{h_1} v_{p'_2} u_{h'_2} \right) \\ V_{p_1 p_2 p'_1 p'_2}^{J,pp} &= \langle (p_1 p_2) J | V_{pp} | (p'_1 p'_2) J \rangle \left( u_{p_1} u_{p_2} u_{p'_1} u_{p'_2} + v_{p_1} v_{p_2} v_{p'_1} v_{p'_2} \right). \end{aligned} \quad (12)$$

In the case at hand, with normal proton and superfluid neutron components, the previous

equations reduce to

$$\begin{aligned} V_{pn'p'n}^{J,ph} &= \langle (pn)J | V_{ph} | (p'n')J \rangle v_n v_{n'} \\ V_{pnp'n'}^{J,pp} &= \langle (pn)J | V_{pp} | (p'n')J \rangle u_n u_{n'}. \end{aligned} \quad (13)$$

The  $|\nu g_{9/2}, \pi g_{7/2}\rangle$  configuration is not very sensitive to the isoscalar pairing, because the associated p-p matrix elements are weighted by factors which include a very small  $u_n$ . On the other hand, the  $u_n$  factors associated with the  $h_{11/2}$  and  $h_{9/2}$  are not so small, and the  $|\nu h_{11/2}, \pi h_{9/2}\rangle$  and  $|\nu h_{9/2}, \pi h_{11/2}\rangle$  configurations have p-p matrix elements larger than the corresponding p-h ones, which are about one half or negligible. Therefore, the  $|\nu h_{9/2}, \pi h_{11/2}\rangle$  is exclusively admixed in the GT wavefunction by the residual (isoscalar) pairing.

By looking also at the neighboring isotope  $^{120}\text{Sn}$ , and comparing with the results obtained with the force SkO', we have reached the following conclusion. Although the presence of the non spin-flip components in the GT wavefunction depends on the p-h interaction (as discussed in Sec. IV), the isoscalar pairing favours this admixture. Moreover, if we increase the strength of the isoscalar pairing force, also more back spin-flip configurations (which are energetically less favoured) mix in the GT wavefunction.

In summary, the effect of pairing (both  $T = 0$  and  $T = 1$  pairing, the latter being responsible for the  $u$  and  $v$  factors) in the resonance region mainly concerns the detailed microscopic structure of the RPA states, besides their individual strength and energy, the GTR centroid energy being less affected and the associated total strength much less. In principle, particle decay experiments could shed light on the microscopic structure of the GTR: quantifying the presence of other components than the pure direct spin-flip ones in the GT wavefunction may highlight the features of corresponding pairing matrix elements. Accordingly, the theoretical framework based on RPA plus the coupling with the continuum and the more complex configurations, which has explained the proton decay from the GTR of  $^{208}\text{Pb}$ , should be extended to superfluid systems. This is left for future work. The present study of the behavior of different Skyrme sets is one of the requirements before going to more ambitious calculations.

We have also checked the effect of isoscalar pairing on the IVSD. The shifts on the  $J^\pi=0^-$ ,  $1^-$  and  $2^-$  centroids, induced by the  $T = 0$  pairing with  $V_0^{(T=0)}$  equal to  $V_0^{(T=1)}$ , amounts to a few hundreds of keV. In  $^{118}\text{Sn}$ , the total IVSD centroid is affected by 500 keV. This effect is not negligible but remains smaller than the variations associated with the choice of the

p-h interaction.

## VII. CONCLUSIONS

In this work, we have tried to shed light on the systematic behavior of the nuclear collective spin-isospin response, in different spherical medium-heavy nuclei, calculated by using the microscopic Skyrme functionals. Our model is a self-consistent QRPA based on HF-BCS, and we have studied both the Gamow-Teller and the spin-dipole strength distributions. We believe that the importance of our work stems from the fact that constraining the microscopic functionals in the spin-isospin channel is highly desirable if studies of exotic nuclei and applications for particle physics or astrophysics are envisaged, in which the spin-isospin transitions must be accurately obtained.

Pairing must be considered if the study has to be extended to different systems for which experimental measurements are available. The resonance properties depend of course mainly on the p-h interaction. We have not only elucidated the features of the existing functionals, but also made suggestions for future fits. In fact, the Lyon force SLy5 does not predict the correct GT collectivity. The other forces we have considered more or less reproduce this collectivity (within our mean field approximation), SGII and SIII overpredicting somehow the GT centroid and SkO' lying closer to it. We have found a clear correlation between the GT collectivity and either selected combinations of Skyrme parameters, or Landau parameters. These correlations may be used to improve the existing Skyrme parametrizations.

The IVSD has been systematically studied using our microscopic QRPA. No such study is available in the literature so far. The IVSD behavior does not introduce new constraints but somewhat confirms what has been deduced from the study of the GTR.

Finally, we have also singled out the effect of pairing (mainly its contribution to the residual proton-neutron interaction). Its effect is not large enough to alter the conclusions which have been drawn concerning the interaction in the p-h channel. However, some conclusions of this part are also interesting. Even if pairing does not affect so much the GT centroid and collectivity, it induces specific admixtures in the wavefunctions. If experimental evidences, coming e.g. from the particle decay, were available, we could say that the microscopic structure of the collective spin-isospin states may help to pin down the features of the effective proton-neutron force in the p-p channel, which is one of the open questions

in nuclear structure.

### **Acknowledgments**

We would like to thank M. Bender for useful communications about his work on the present subject, as well as H. Sagawa, N. Van Giai and R. Zegers for helpful discussions.

## APPENDIX: EXPLICIT FORM OF THE RESIDUAL P-H INTERACTION

The coefficients appearing in Eq. (6) are

$$\begin{aligned}
C_1^\rho[\rho] &= -\frac{1}{8}(t_0 - 2t_0x_0) - \frac{1}{48}\rho^\alpha(t_3 + 2t_3x_3), \\
C_1^S[\rho] &= -\frac{t_0}{8} - \frac{t_3}{48}\rho^\alpha, \\
C_1^\tau &= \frac{1}{64}(-4t_1 - 8t_1x_1 + 4t_2 + 8t_2x_2), \\
C_1^{\Delta\rho} &= \frac{1}{64}(3t_1 + 6t_1x_1 + t_2 + 2t_2x_2), \\
C_1^T &= \frac{1}{16}(-t_1 + t_2), \\
C_1^{\Delta S} &= \frac{1}{64}(3t_1 + t_2), \\
C_1^{\nabla J} &= -\frac{1}{4}W_0
\end{aligned} \tag{14}$$

(in the case in which the spin-orbit part of the functional is generalized by introducing the parameters  $b_4$  and  $b'_4$  [47], the last expression becomes  $-\frac{1}{2}b'_4$ ). If we insert these expressions in (6) we find

$$\begin{aligned}
v_{01}(r) &= \left[ 2\left(-\frac{t_0}{8} - \frac{1}{4}t_0x_0\right) - \frac{1}{24}\rho^\alpha(r)(t_3 + 2t_3x_3) \right] \vec{\tau}_1 \vec{\tau}_2, \\
v_{11}(r) &= \left[ -\frac{t_0}{4} - \frac{t_3}{24}\rho^\alpha(r) \right] \vec{\sigma}_1 \vec{\sigma}_2 \vec{\tau}_1 \vec{\tau}_2, \\
v'_{01} &= \left[ -\frac{t_1}{8}(2x_1 + 1)(k'^2 + k^2) + \frac{t_2}{4}(2x_2 + 1)(k'k) \right] \vec{\tau}_1 \vec{\tau}_2, \\
v'_{11} &= \left[ -\frac{t_1}{8}(k'^2 + k^2) + \frac{t_2}{4}k'k \right] \vec{\sigma}_1 \vec{\sigma}_2 \vec{\tau}_1 \vec{\tau}_2, \\
v_1^{(s.o.)} &= \frac{iW_0}{2}(\sigma_1 + \sigma_2)k' \times k \vec{\tau}_1 \vec{\tau}_2,
\end{aligned} \tag{15}$$

keeping the same notation of Sec. II.

The choice of neglecting the contribution to the residual interaction from the  $J^2$  terms amounts to writing

$$\begin{aligned}
v'_{01} &= \left[ \frac{1}{16}[\nabla_1 \nabla_2 + \nabla'_1 \nabla'_2](2x_1 t_1 - t_1) + \frac{1}{4}k'k(2x_2 t_2 + t_2) \right] \vec{\sigma}_1 \vec{\sigma}_2, \\
v'_{11} &= \left[ -\frac{t_1}{16}[\nabla_1 \nabla_2 + \nabla'_1 \nabla'_2] + \frac{t_2}{4}k'k \right] \vec{\tau}_1 \vec{\tau}_2 \vec{\sigma}_1 \vec{\sigma}_2.
\end{aligned} \tag{16}$$

As mentioned in Sec. II, it is appropriate to give here the expressions for the Landau parameters discussed in the paper. In symmetric nuclear matter, the  $\ell=0$  and 1 spin-isospin

parameters are

$$\begin{aligned} g'_0 &= -N_0 \left[ \frac{1}{4}t_0 + \frac{1}{24}t_3\rho^\alpha + \frac{1}{8}k_F^2(t_1 - t_2) \right] \\ g'_1 &= N_0 \left( \frac{t_1}{8} - \frac{t_2}{8} \right) k_F^2, \end{aligned} \quad (17)$$

where  $N_0 = 2k_F m^* / \pi^2 \hbar^2$  and  $k_F$  is the Fermi momentum. The Landau parameters are zero for  $\ell > 1$ . If we re-write the Landau parameters in terms of the coefficients of Eq. (6), they read

$$\begin{aligned} g'_0 &= N_0 \left( 2C_1^S + 2C_1^T k_F^2 \right), \\ g'_1 &= -2N_0 C_1^T k_F^2. \end{aligned} \quad (18)$$

---

[1] F. Osterfeld, Rev. Mod. Phys. 64, 491 (1992).

[2] M.N. Harakeh and A. Van Der Woude, *Giant Resonances. Fundamental High-Frequency Modes of Nuclear Excitation* (Clarendon Press, Oxford, 2001).

[3] K. Ikeda, S. Fuji and J.I. Fujita, Phys. Lett. 3, 271 (1963).

[4] R.R. Doering, A. Galonsky, D.R. Patterson, G.F. Bertsch, Phys. Rev. Lett. 35, 1691 (1975).

[5] J. Rapaport *et al.*, Nucl. Phys. A410, 371 (1983); C. Gaarde, in *Proceedings of the Niels Bohr Centennial Conference on Nuclear Structure*, Copenhagen (North-Holland, Amsterdam), p. 449c.

[6] C.D. Goodman *et al.*, Phys. Rev. Lett. 44, 1755 (1980); T.N. Taddeucci *et al.*, Nucl. Phys. A469, 125 (1987).

[7] G.F. Bertsch and I. Hamamoto, Phys. Rev. C26, 1323 (1982); S. Drozdz *et al.*, Phys. Lett. B189, 271 (1987).

[8] T. Wakasa *et al.*, Phys. Rev. C55, 2909 (1997).

[9] G. Colò, N. Van Giai, P.F. Bortignon, R.A. Broglia, Phys. Rev. C50, 1496 (1994).

[10] Nguyen Ding Dang *et al.*, Phys. Rev. Lett. 79, 1638 (1997).

[11] S. Fracasso and G. Colò, Phys. Rev. C72, 064310 (2005).

[12] S. Fracasso and G. Colò, in *Frontiers in nuclear structure, astrophysics and reactions* (FL-NUSTAR, Kos, Greece, September 2005), S.V. Harissopoulos, P. Demetriou and R. Julin Eds. (AIP Conference Proceedings Series, vol. 831, Melville, New York, 2006); S. Fracasso and G. Colò, *Yad. Fiz.* (to be published).

[13] P. Sarriuguren *et al.*, Nucl. Phys. A635, 55 (1998); Nucl. Phys. A658, 13 (1999); Nucl. Phys. A691, 631 (2001); Phys. Rev. C64, 064306 (2001).

[14] O. Moreno *et al.*, Phys. Rev. C73, 054302 (2006).

[15] J. Engel, M. Bender, J. Dobaczewski, W. Nazarewicz and R. Surman, Phys. Rev. C60, 014302 (1999).

[16] M. Bender, J. Dobaczewski, J. Engel and W. Nazarewicz, Phys. Rev. C65, 054322 (2002).

[17] C. De Conti *et al.*, Phys. Lett. B444, 14 (1998); Phys. Lett. B494, 46 (2000).

[18] N. Paar, T. Nikšić, D. Vretenar and P. Ring, Phys. Rev. C69, 054303 (2004).

[19] Z-Y. Ma, B-Q. Chen, N. Van Giai, and T. Suzuki, Eur. Phys. J. A20, 429 (2004).

- [20] P. Finelli, Nucl. Phys. A (in press).
- [21] V.A. Kuzmin and V.G. Soloviev, J. Phys. G10, 1507 (1984).
- [22] T. Babacan, D.I. Salamov and A. Kücükbursa, Phys. Rev. C71, 037303 (2005).
- [23] G. Bertsch, D. Cha, H. Toki, Phys. Rev. C24, 533 (1981).
- [24] N. Auerbach and A. Klein, Phys. Rev. C30, 1032 (1984).
- [25] A. Krasznahorkay *et al.*, Phys. Rev. Lett. 82, 3216 (1999).
- [26] H. Sagawa *et al.*, to be published; H. Sagawa (private communication).
- [27] M. Beiner, H. Flocard, N. Van Giai and Ph. Quentin, Nucl. Phys. A238, 29 (1975).
- [28] N. Van Giai and H. Sagawa, Phys. Lett. B106, 379 (1981).
- [29] E. Chabanat, P. Bonche, P. Haensel, J. Meyer, R. Schaeffer, Nucl. Phys. A635, 231 (1998).
- [30] P.-G. Reinhard, D.J. Dean, W. Nazarewicz, J. Dobaczewski, J.A. Maruhn and M.R. Strayer, Phys. Rev. C60, 014316 (1999).
- [31] N. Auerbach and A. Klein, Nucl. Phys. A395 (1983) 77.
- [32] D. Vautherin and D.M. Brink, Phys. Rev. C5, 626 (1972).
- [33] G. Colò, H. Sagawa, S. Fracasso, P.F. Bortignon, Phys. Lett. B646 (2007) 227.
- [34] J. Dobaczewski, nucl-th/0604043, D.M. Brink, Fl. Stancu, nucl-th/0702065.
- [35] K. Pham *et al.*, Phys. Rev. C51, 526 (1995).
- [36] H. Akimune *et al.*, Phys. Rev. C52, 604 (1995).
- [37] A. Krasznahorkay *et al.*, Phys. Rev. C64, 067302 (2001).
- [38] K. Nakayama, A. Pio Galeão, F. Krmpotić, Phys. Lett. B114, 217 (1982).
- [39] C. Gaarde, J. Rapaport, T.N. Taddeucci, C.D. Goodman, C.C. Foster, D.E. Bainum, C.A. Goulding, M.B. Greenfield, D.J. Horen, E. Sugarbaker, Nucl. Phys. A369, 258 (1981).
- [40] T. Suzuki and H. Sagawa, Eur. Phys. J. A9, 49 (2000).
- [41] M. Bender (private communication).
- [42] M.N. Harakeh, Acta Phys. Pol. B29, 2199 (1998).
- [43] H. Akimune, I. Daito, Y. Fujita, M. Fujiwara, M.N. Harakeh, J. Jänecke, M. Yosoi, Phys. Rev. C61, 011304R (1999).
- [44] D.J. Horen, C.D. Goodman, C.C. Foster, C.A. Goulding, M.B. Greenfield, J. Rapaport, D.E. Bainum, E. Sugarbaker, T.G. Masterson, F. Petrovich, W.G. Love, Phys. Lett. B95, 27 (1980).
- [45] R. Zegers, in *COLlective Motion in nuclei under EXtreme conditions* (COMEX2, Sankt Goar, Germany, June 2006), Nucl. Phys. A (in press) and references therein.

	$^{114}\text{Sn}$	$^{118}\text{Sn}$	$^{120}\text{Sn}$	$^{124}\text{Sn}$	$^{208}\text{Pb}$
SIII	60.44	60.98	61.44	62.76	60.68
SGII	61.75	61.30	61.49	63.36	67.24
SLy5	46.38	42.06	41.16	41.41	44.76
SKO'	66.06	67.08	67.19	72.76	79.80

TABLE I: Percentages of the Ikeda sum rule  $m_0$  exhausted in the giant resonance region. This region is 12-22 MeV in the Sn isotopes and 15-24 MeV in  $^{208}\text{Pb}$ .

Configuration	Weight
$\nu i_{13/2} \rightarrow \pi i_{11/2}$	0.69
$\nu h_{11/2} \rightarrow \pi h_{9/2}$	0.49
$\nu f_{7/2} \rightarrow \pi f_{5/2}$	0.28
$\nu i_{13/2} \rightarrow \pi i_{13/2}$	0.20
$\nu f_{7/2} \rightarrow \pi f_{7/2}$	0.16
$\nu h_{9/2} \rightarrow \pi h_{9/2}$	0.16
$\nu p_{3/2} \rightarrow \pi p_{1/2}$	0.13
$\nu p_{3/2} \rightarrow \pi p_{3/2}$	0.13
$\nu f_{5/2} \rightarrow \pi f_{5/2}$	0.11
$\nu f_{5/2} \rightarrow \pi f_{7/2}$	0.15
$\nu p_{1/2} \rightarrow \pi p_{3/2}$	0.11

TABLE II: Wavefunction of the main GT state in  $^{208}\text{Pb}$  obtained with the SkO' force. Under the label “weight” we report the absolute value of the quantity  $X_{ph} + (-)^{S(J+L)}Y_{ph}$ , which enter the calculation of the  $B(\text{GT})$  value.

[46] V.G. Guba, M.A. Nikolaev, and M.G. Urin, Phys. Lett. B218, 283 (1989).  
[47] P.-G. Reinhard, H. Flocard, Nucl. Phys. 584, 467 (1995).

Configuration	Weight
$\nu i_{13/2} \rightarrow \pi i_{11/2}$	0.79
$\nu h_{11/2} \rightarrow \pi h_{11/2}$	0.59
$\nu f_{7/2} \rightarrow \pi f_{5/2}$	0.11
$\nu i_{13/2} \rightarrow \pi i_{13/2}$	0.04

TABLE III: Same as the previous Table, in the case of the SLy5 force.

$J^\pi$	$m_{J^\pi}(0)$ [fm $^2$ ]	$m_{J^\pi}(1)/m_{J^\pi}(0)$ [MeV]
$0^-$	147.9 (162.5)	28.21 (20.16)
$^{208}\text{Pb}$	1 $^-$	467.9 (436.0)
	2 $^-$	650.0 (667.0)
	Tot.	1265.8 (1265.5)
		23.18 (16.67)
$0^-$	57.6 (65.9)	26.82 (20.11)
$^{120}\text{Sn}$	1 $^-$	207.3 (179.5)
	2 $^-$	235.2 (256.5)
	Tot.	500.2 (501.9)
		22.47 (16.55)

TABLE IV: (Q)RPA (HF-BCS) summed transition strengths, and centroid energies, for the three spin-dipole components. The total centroid defined by Eq. (11) is also reported. All results correspond to the SkO' force, as in Figs. 10 and 11.

$J^\pi$	$m_{J^\pi}(0)$ [fm $^2$ ]	$m_{J^\pi}(1)/m_{J^\pi}(0)$ [MeV]
0 $^-$	158.8 (159.8)	29.84 (23.30)
$^{208}\text{Pb}$ 1 $^-$	432.7 (428.0)	27.21 (21.16)
2 $^-$	645.8 (653.2)	21.25 (16.14)
Tot.		1237.3 (1241.1) 24.44 (18.79)
0 $^-$	64.8 (66.5)	28.31 (22.17)
$^{120}\text{Sn}$ 1 $^-$	187.7 (181.4)	25.72 (20.08)
2 $^-$	249.7 (257.9)	20.83 (15.93)
Tot.		502.1 (505.9) 23.63 (18.24)

TABLE V: The same as Table IV in the case of the SLy5 force.

Energy (percentage of $m_0$ )	Configuration	Weight
15.25 MeV (26.4%)	$\nu g_{9/2}, \pi g_{7/2}$	0.93
16.49 MeV (9.7%)	$\nu d_{5/2}, \pi d_{3/2}$	0.07
18.59 MeV (6.0%)	$\nu h_{11/2}, \pi h_{9/2}$	0.31
	$\nu g_{9/2}, \pi g_{7/2}$	0.30
	$\nu h_{11/2}, \pi h_{9/2}$	0.62
	$\nu h_{11/2}, \pi h_{11/2}$	0.11
	$\nu h_{9/2}, \pi h_{11/2}$	0.67
	$\nu g_{9/2}, \pi g_{7/2}$	0.15
	$\nu h_{11/2}, \pi h_{9/2}$	0.68
	$\nu h_{9/2}, \pi h_{11/2}$	0.69

TABLE VI: Wavefunctions of the QRPA states obtained for the GTR in  $^{118}\text{Sn}$ , with the interaction SLy5, when the isoscalar residual pairing is included and its strength is set equal to that of the isovector pairing (namely 680 MeV·fm $^3$ ).

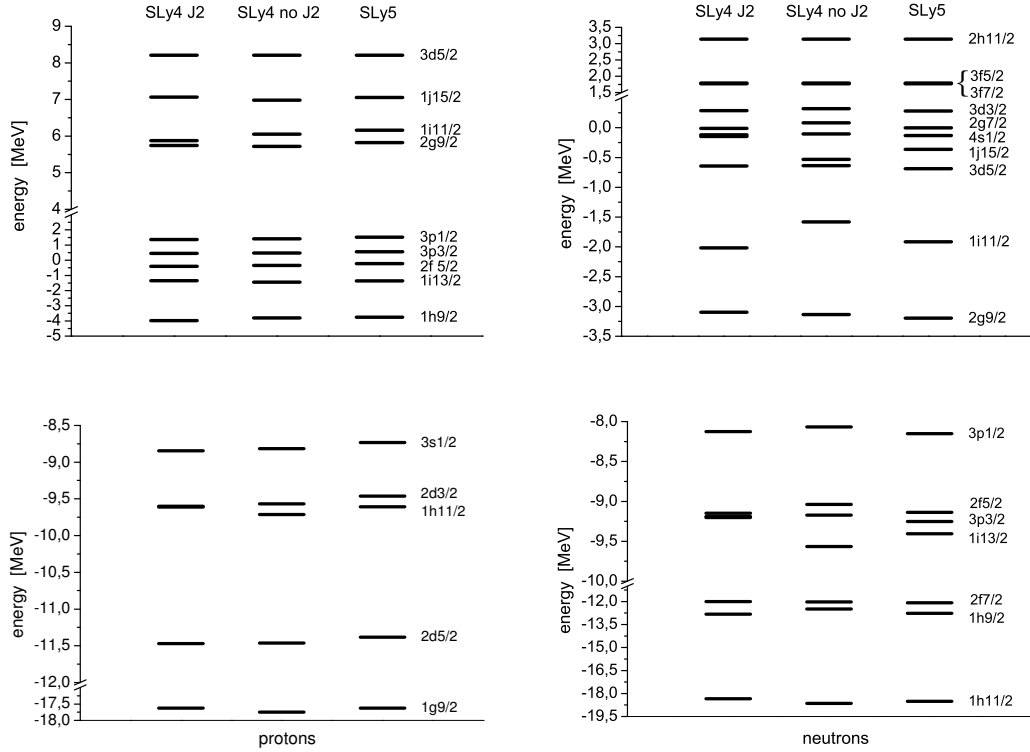


FIG. 1: Single-particle levels of  $^{208}\text{Pb}$ , calculated using Skyrme-HF and employing respectively the parametrization SLy4 with and without the  $J^2$  terms and the parametrization SLy5. The left (right) part refers to protons (neutrons). The lower (upper) panel includes levels below (above) the Fermi energy.

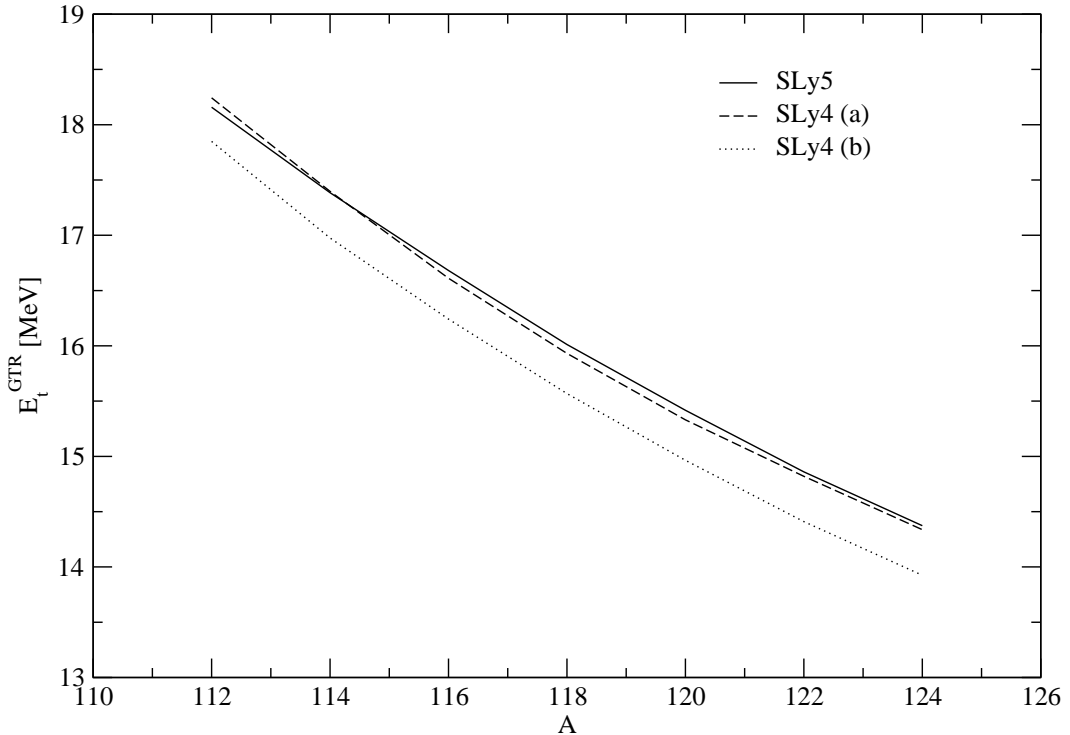


FIG. 2: GTR peak energies, along the Sn isotope chain, calculated by using either the force SLy5 (full line) or the force SLy4 with (dotted line) and without (dashed line) the contribution associated with the  $J^2$  terms in the mean field. See the text for the discussion.

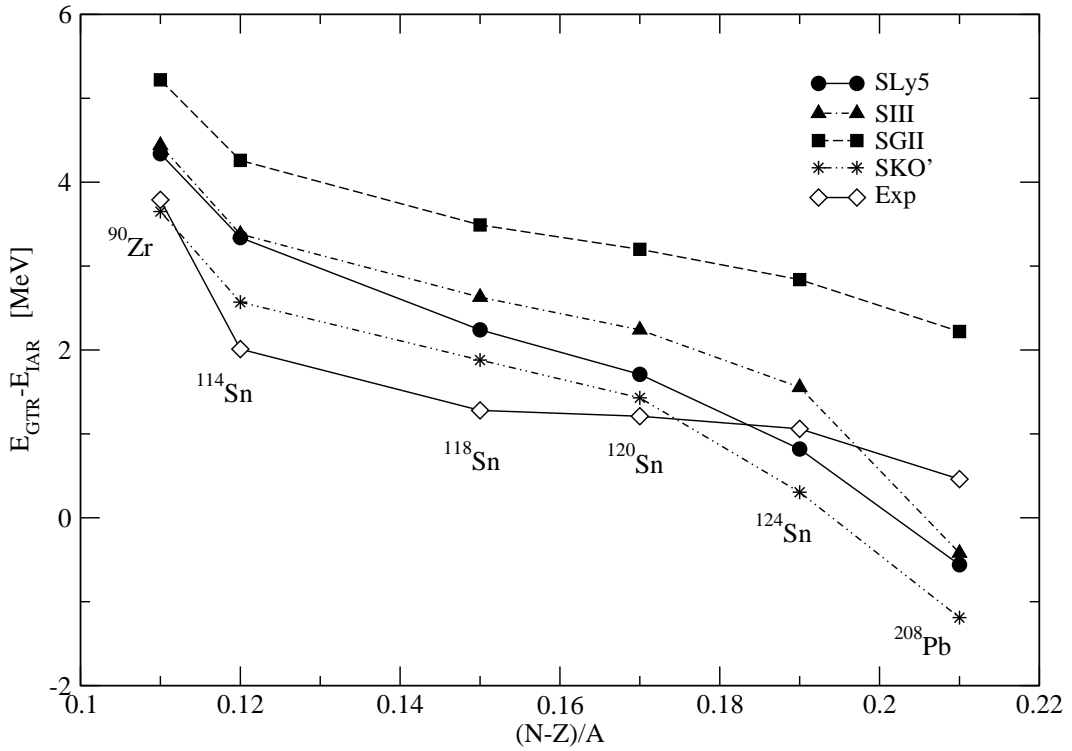


FIG. 3: Difference between the GTR and the IAR energies in some selected spherical nuclei as a function of  $(N - Z)/A$ . Theoretical results associated with different Skyrme parametrizations are compared with experimental values from Refs. [35, 36, 37]. The related discussion, including details on how the energies have been defined, can be found in the text.

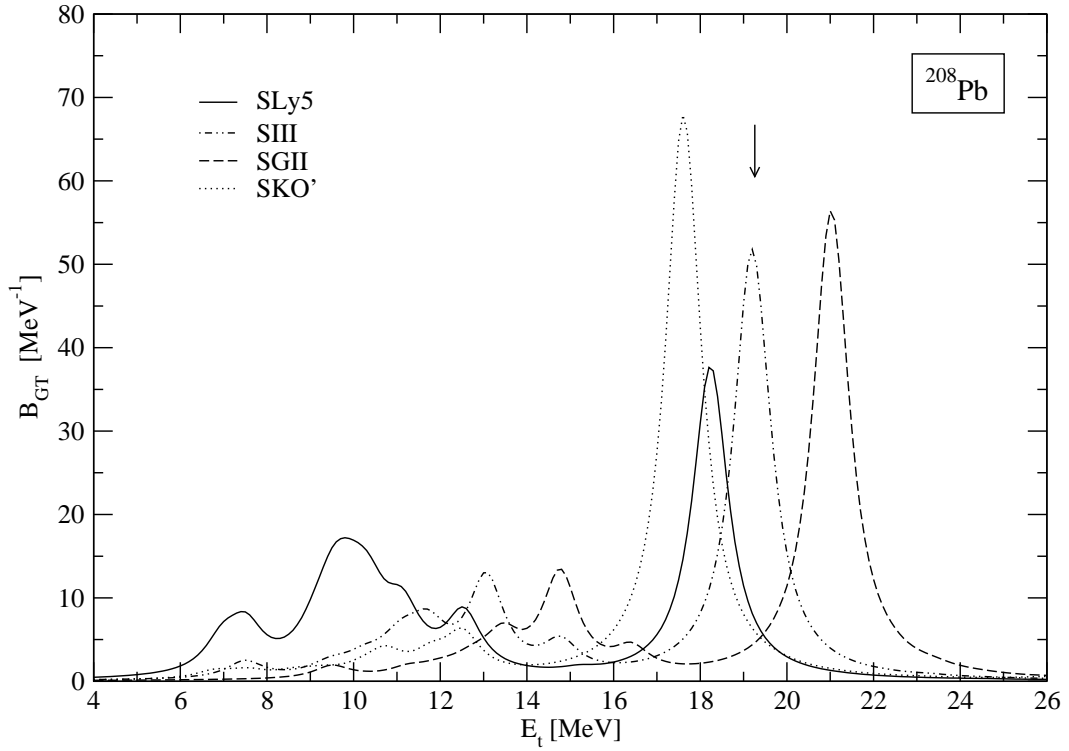


FIG. 4: Gamow-Teller strength distributions in  $^{208}\text{Pb}$ , calculated using different Skyrme forces within HF plus RPA. The results are displayed as function of the energy in the target nucleus ( $E_t$ ). The discrete RPA peaks have been smeared out using Lorentzian functions having 1 MeV width. The arrow corresponds to the experimental energy.

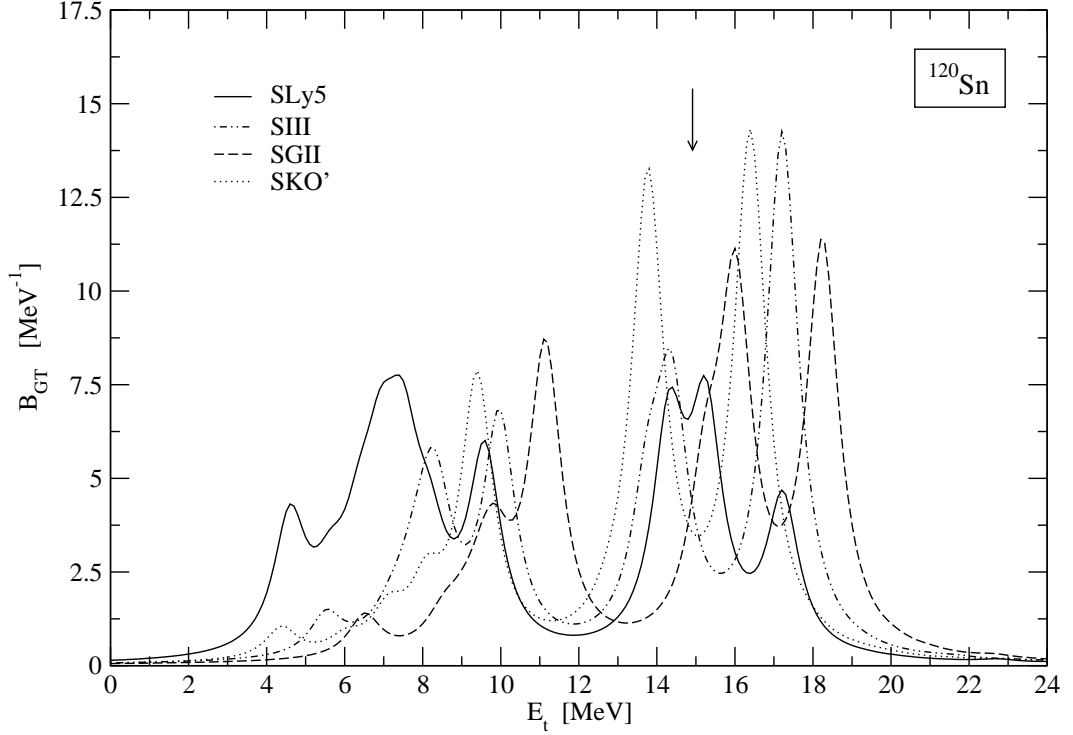


FIG. 5: Same as Fig. 4 for the open-shell nucleus  $^{120}\text{Sn}$ .

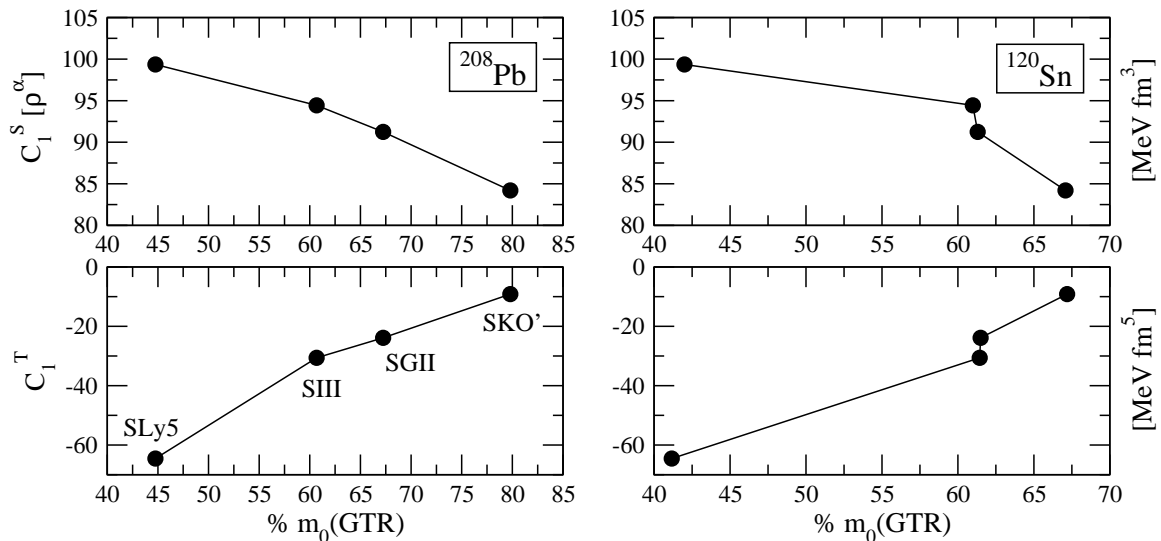


FIG. 6: Correlations between relevant parameters of the residual p-h interaction (cf. Eq. (6)) and the percentage of  $m_0$  exhausted by the GTR. The left (right) panel refer to  $^{208}\text{Pb}$  ( $^{120}\text{Sn}$ ). In the upper part of the figure, the coefficient  $C_1^S$  has been evaluated at  $\rho=0.16 \text{ fm}^{-3}$ .

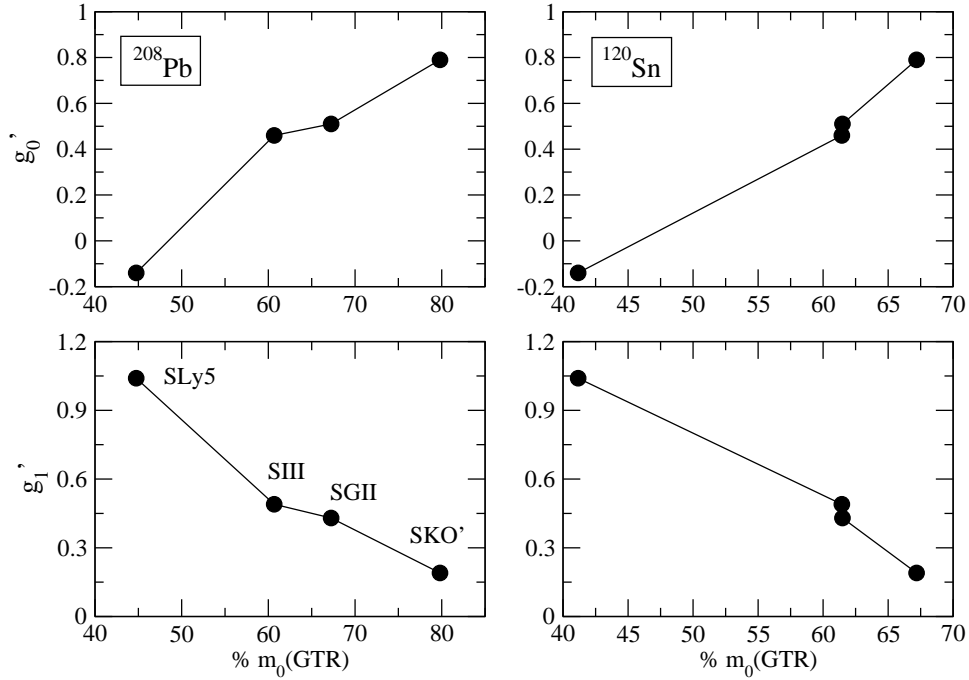


FIG. 7: Correlations between the Landau parameters  $g'_0$  or  $g'_1$  and the percentage of  $m_0$  exhausted by the Gamow-Teller resonance. The left (right) panel refer to  $^{208}\text{Pb}$  ( $^{120}\text{Sn}$ ).

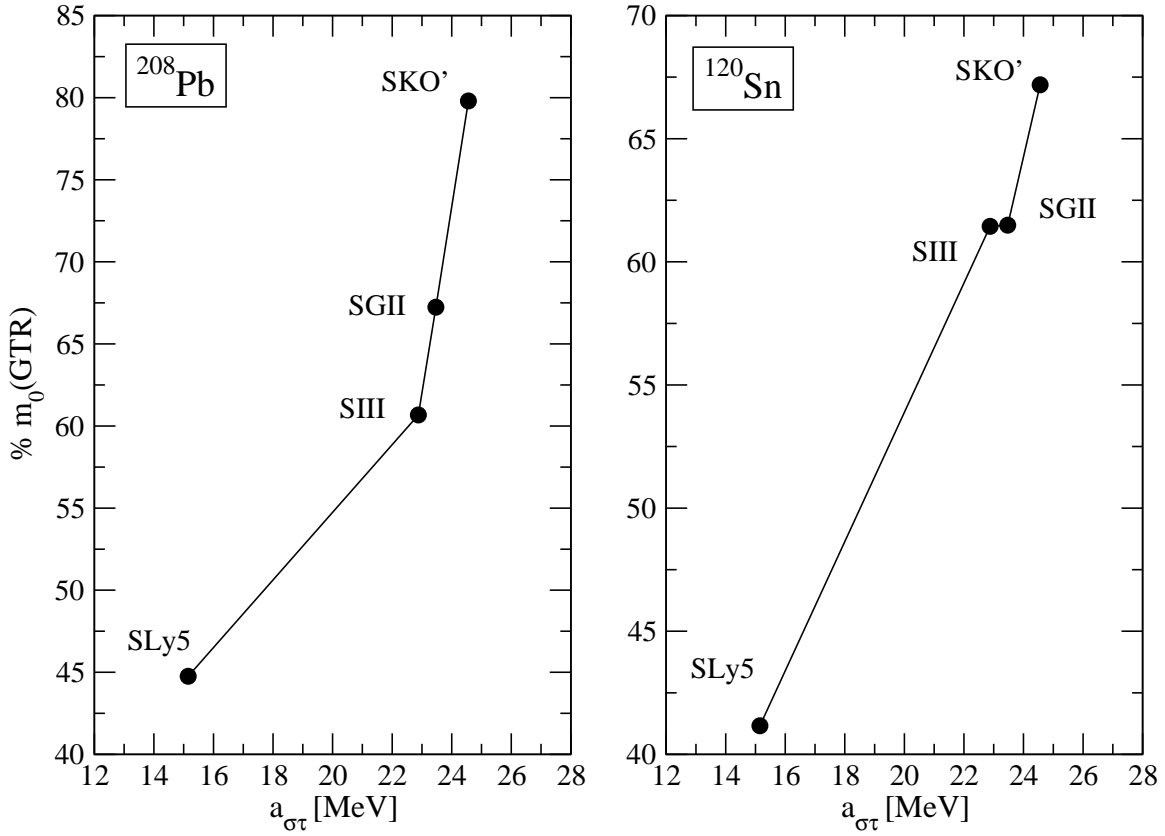


FIG. 8: Correlation between the parameter  $a_{\sigma\tau}$  defined in the text and the percentage of  $m_0$  exhausted by the Gamow-Teller resonance. The left (right) panel refer to  $^{208}\text{Pb}$  ( $^{120}\text{Sn}$ ).

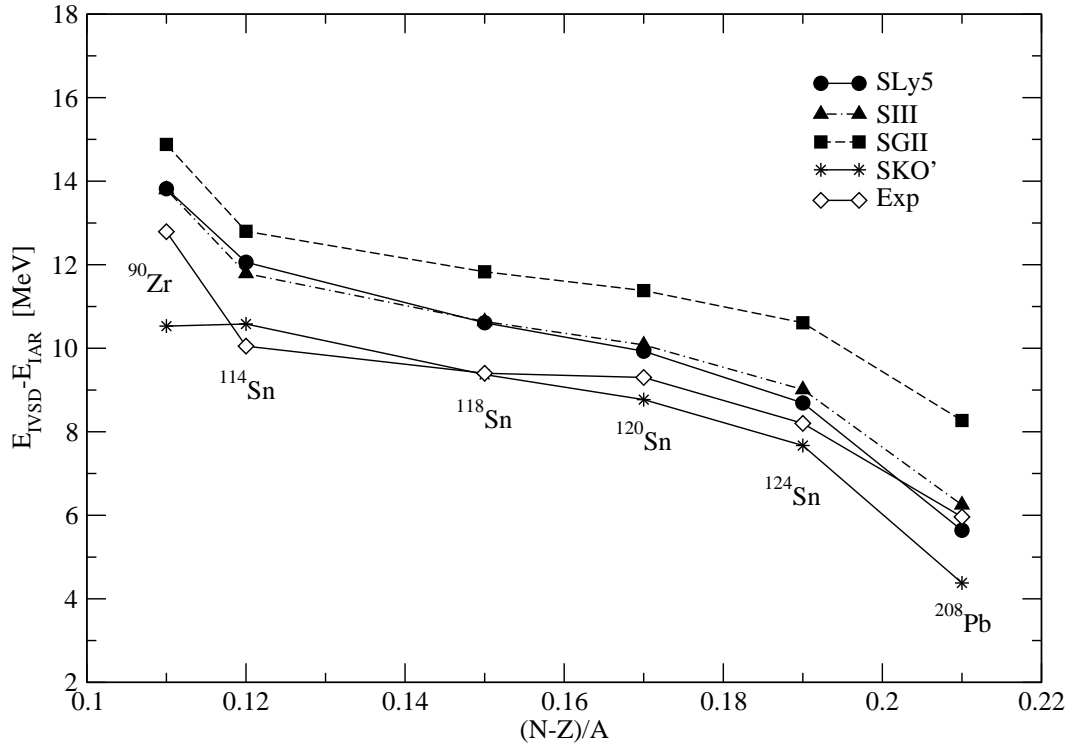


FIG. 9: Same as Fig. 3 for the spin-dipole case, that is, difference between the IVSD and the IAR energies in some selected spherical nuclei as a function of  $(N - Z)/A$ . Experimental data are from Refs. [25, 39, 43].

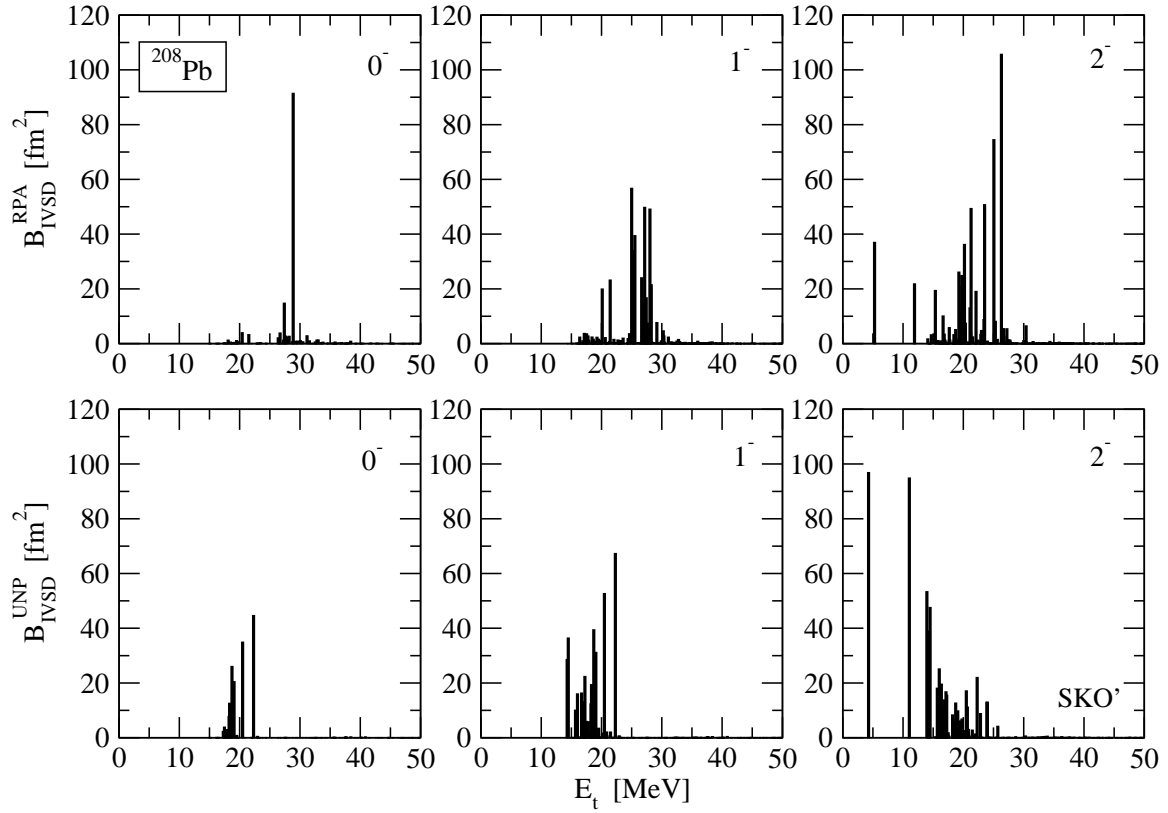


FIG. 10: RPA (upper panels) and unperturbed (lower panels) strength distributions for the three spin components of the IVSD. They are calculated using the force SkO' in the nucleus  $^{208}\text{Pb}$ .

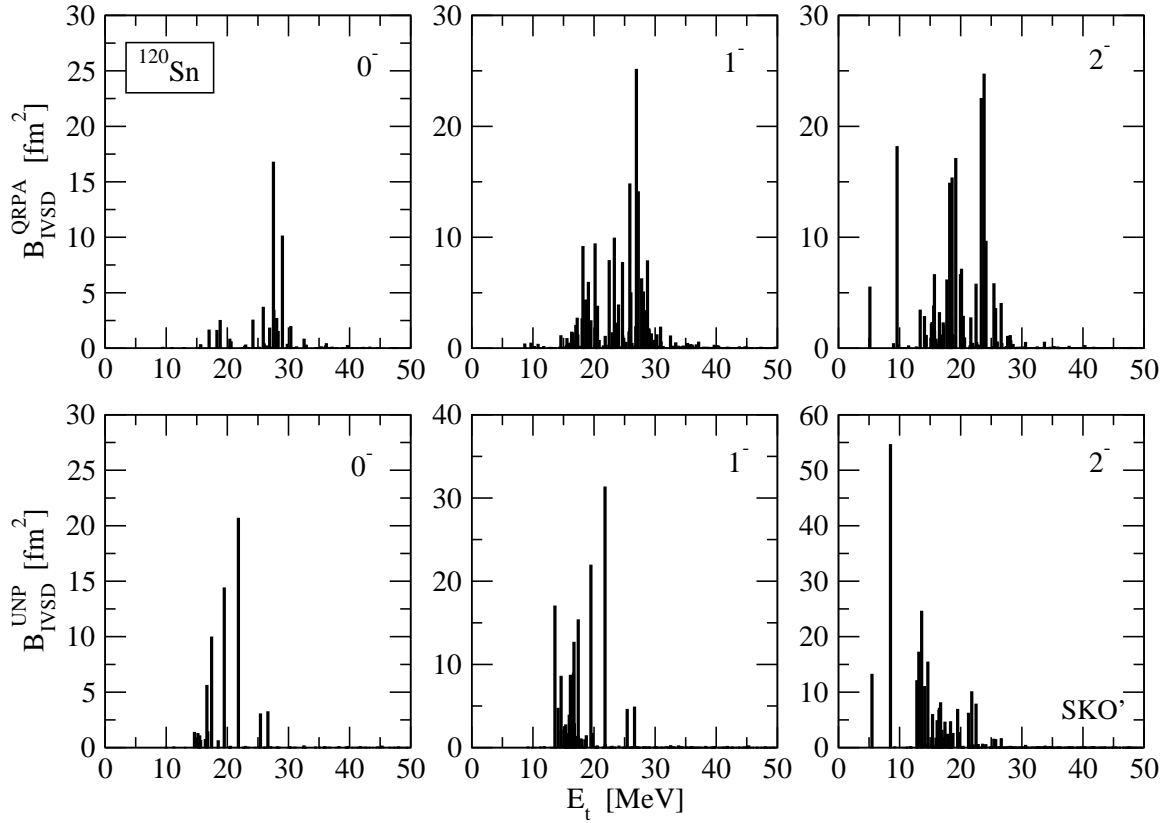


FIG. 11: QRPA (upper panels) and unperturbed (lower panels) strength distributions for the three spin components of the IVSD. They are calculated using the force SkO' in the nucleus  $^{120}\text{Sn}$ .

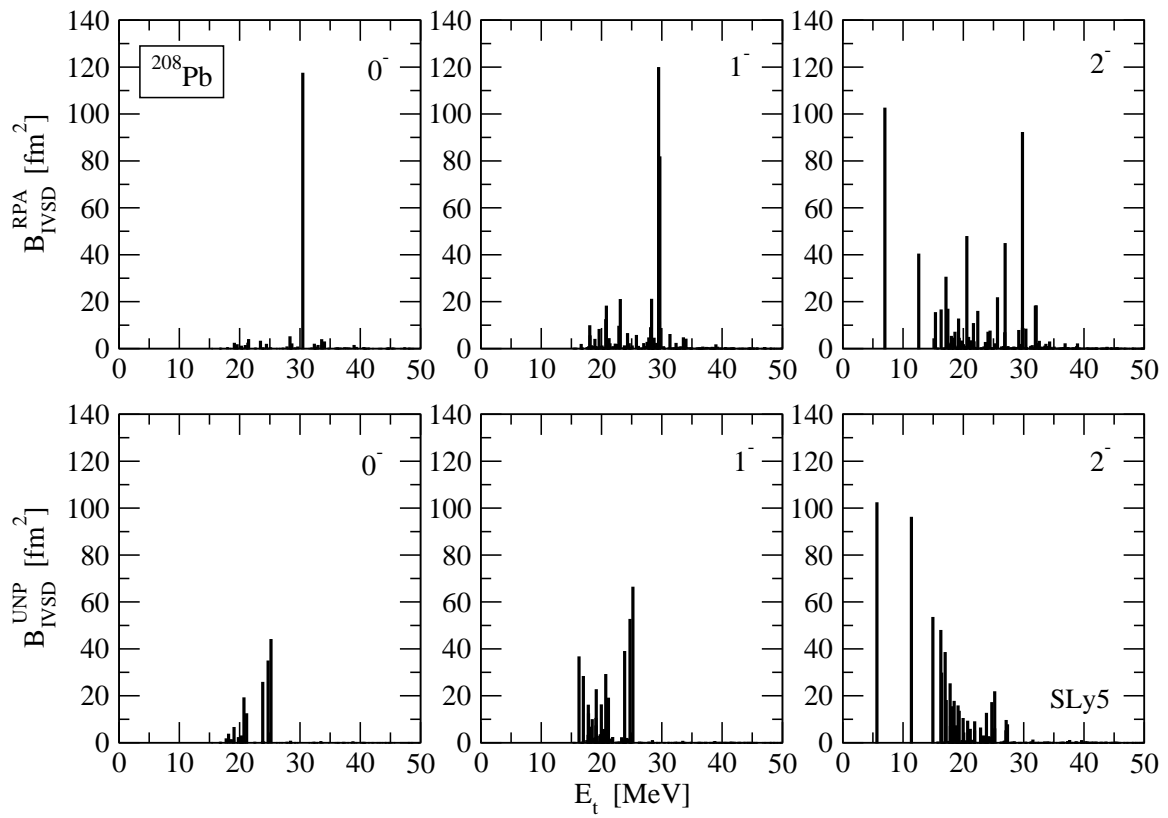


FIG. 12: The same as Fig. 10 in the case of the force SLy5.

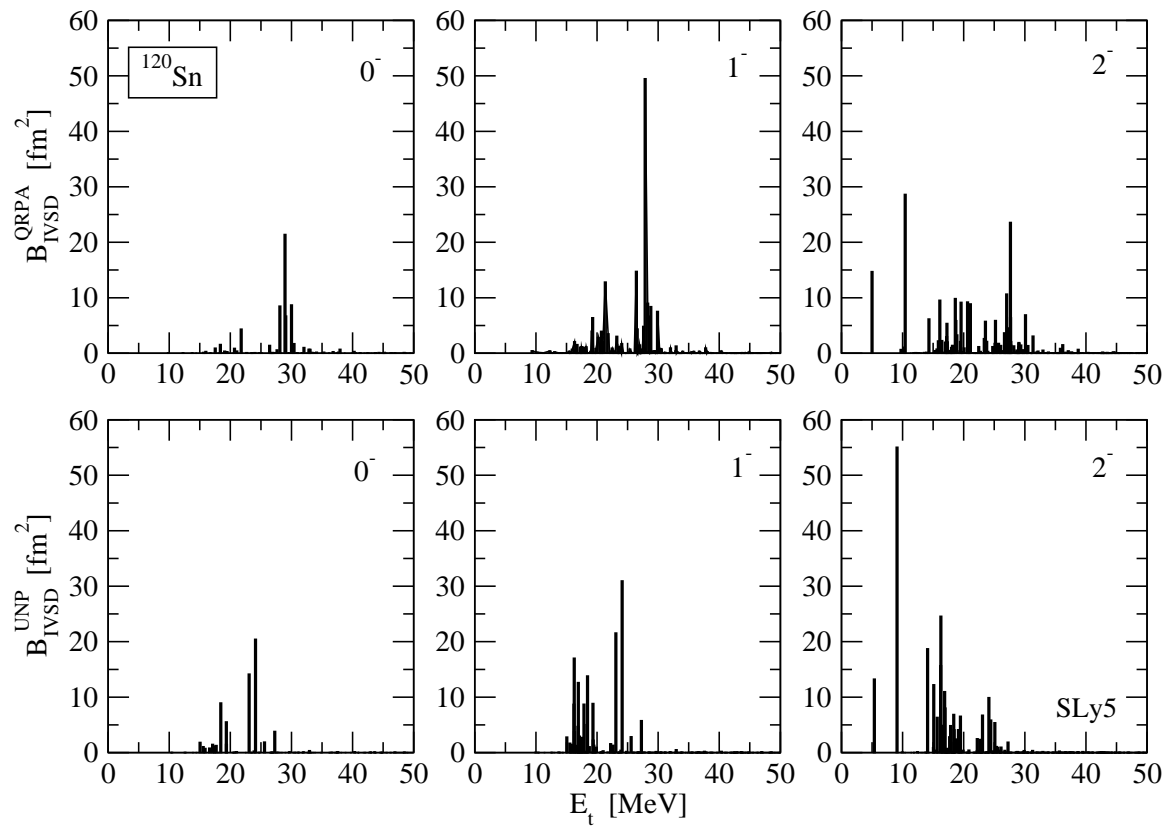


FIG. 13: The same as Fig. 11 in the case of the force SLy5.

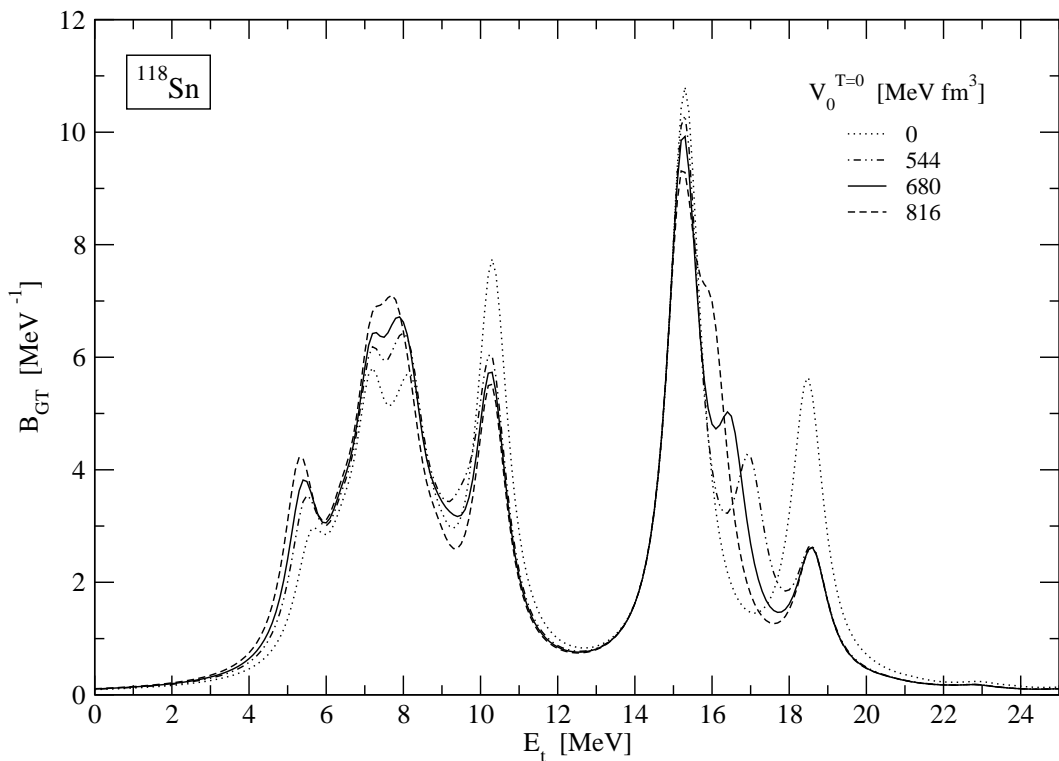


FIG. 14: GT strength distributions obtained in the nucleus  $^{118}\text{Sn}$  by using the force SLy5 and varying the strength of the residual p-p isoscalar force.